A Laser Tomography Test Bed For Extremely Large Telescope

R. Conan[a], P. Piatrou[a], F. Rigaut[a] and K. Uhlendorf[b]

[a]RSAA, The Australian National University, Weston Creek, ACT 2611, Australia [b] Germany

ABSTRACT

The Advanced Instrumentation and Technology Center at the Australian National University is building a Laser Tomography Adaptive Optics Test Bed for Extremely Large Telescopes. The optical test bench is using three Laser Guide Stars (LGS) propagating through three phase screens. The LGS wavefronts are sampled with a 16×16 Shack–Hartmann wavefront sensor (SH–WFS). Cone effect, spot elongation and Sodium layer density fluctuations are reproduced on the bench. Two Natural Guide Stars (NGS), on–axis and off–axis, are also added to the bench. The wavefront of the on–axis NGS is corrected with a DM located in the optical path of both the LGSs and the on–axis NGS. The DM commands are derived from the tomographic estimate of the on–axis NGS wavefront using the measurements of the 3 LGS WFSs. The off-axis NGS wavefront is sampled with a 6×6 SH–WFS and is emulating tip–tilt, focus and truth sensing. A DM located in front of the off-axis NGS WFS is correcting the off-axis NGS wavefront. The commands of this DM are also derived from the tomographic reconstructor. In the paper, the design of the LTAO test bed is presented.

Keywords: adaptive optics, wavefront sensing, atmospheric turbulence

1. INTRODUCTION

A laboratory based demonstrator[1–3] of any complex AO system is an indispensable tool to validate the choices made during the design phase. Such demonstrator allows comparing the performance of algorithms, to assess hardware, to debug software, to train staff, etc. Compared to computer simulations, a demonstrator brings the system one step closer to real life situations confronting the design to the sometimes unforeseen limitation of hardware components. At the Research School of Astronomy and Astrophysics of the Australian National University, a LTAO optical test bed is going to be built in the optics laboratory. The bench is intended to mimic many aspects of the LTAO system of the Giant Magellan Telescope[4] (GMT).

The LTAO test bench will be used to perform the following tasks:

Tomography: assessing both on–axis and off–axis tomography algorithms performance,

Laser Guide Star wavefront sensing: comparison of centroiding algorithm in presence of Na layer fluctuations, atmosphere aberrations, read-out and photon noise,

C_n^2 **profiling:** assessing different algorithms to estimate the atmosphere profile,

Truth sensing: assessing truth sensor control algorithms,

Phasing of segmented pupil: validation of proposed phasing techniques for the GMT,[5]

Focus control: assessing control algorithms for the tracking of the Na layer mean altitude,

LGS jitter loop: assessing control algorithms for tracking the Laser guide stars,

Pupil tracking: assessing the accuracy of pupil tracking algorithms.

Further author information: (Send correspondence to R. Conan)
R. Conan: E-mail: rod.conan@anu.edu.au

Adaptive Optics Systems IV, edited by Enrico Marchetti, Laird M. Close, Jean-Pierre Véran, Proc. of SPIE Vol. 9148, 91485T · © 2014 SPIE
CCC code: 0277-786X/14/$18 · doi: 10.1117/12.2054471

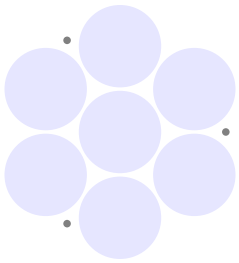

Figure 1. The GMT pupil with the location of the launch telescope.

2. TOP LEVEL REQUIREMENTS

2.1 Laser Guide Star

2.1.1 Number

The AO bench must used at least 3 LGSs.

2.1.2 Na profile

The AO bench must reproduce the effects of the Na layer (thickness and Na density time fluctuations) on a Shack–Hartmann WFS.

2.1.3 LGS jitter

The AO bench should reproduce the effect of the Laser uplink propagation through the atmosphere.

2.1.4 Cone effect

The AO bench should reproduce the cone effect.

2.1.5 Launch telescope

The AO bench must reproduce the WFS spot elongation corresponding to LGSs launched from the telescope edge.

2.2 Atmosphere

The AO bench must have an atmosphere simulator with at least 3 atmospheric layers.

2.3 Natural Guide Star

The AO bench should use 2 NGSs, one on–axis and one off–axis.

2.4 On–axis correction

The AO bench must employ a DM for the correction of the on–axis NGS. The DM must also provide a partial correction for the LGS and the off–axis NGS.

2.5 Off–axis correction

The off–axis NGS should be corrected with a dedicated deformable mirror.

2.6 Pupil

The pupil should be segmented with a ratio between segment gap and segment diameter similar to the GMT pupil(Fig. 1). A deformable mirror must be located in a pupil plane to emulate the GMT ASM.

3. DETAILED REQUIREMENTS

3.1 Atmosphere model

The standard GMT atmosphere model is a 7 layers model with a $r_0(500\text{nm}) = 15.1\text{cm}$ and $\mathcal{L}_0 = 60\text{m}$. The GMT LGS WFS will operate at 589nm. On the bench there is no need to operate at this wavelength, so we will use a standard Laser diode at $\lambda_{lab} = 635\text{nm}$, leading to $r_0(\lambda_{lab}) = 20\text{cm}$ For the GMT, the pitch of the WFS is $d = 43\text{cm}$ giving a $d/r_0(\lambda_{lab}) = 2.15$. In order to get a similar fitting error for the laboratory experiment, the same d/r_0 should be used. The effect of the atmosphere on the system performance depends also on the ratio $D/\mathcal{L}_0 = 0.43$ for the GMT. The same $D/\mathcal{L}_0$ ratio should be achieved on the bench.

The bench atmosphere model should have also similar θ_0 and τ_0 compared to the GMT standard atmosphere.

3.2 Laser Guide Stars

The SH–WFS spot elongation is well approximated with

$$\theta_{Na} = L\delta_{Na}/h_{Na}^2$$

with δ_{Na} and h_{Na} the Na layer thickness and distance to the Na layer from the telescope pupil, respectively, and L the distance from the launch telescope to the lenslet. The LGS must reproduce the spot elongation as seen on the GMT when they are launched from the telescope edges i.e. $\theta_{Na} = 10.72$" for $L = 24.0745\text{m}$, $\delta_{Na} = 17.5\text{km}$ and $h_{Na} = 90\text{km}$.

The non–elongated spot size is expected to be around $\theta_{LGS} = 1$". On the bench, the non elongated spot size is given by the lenslet diffraction limit, i.e. $\theta_{LGS} = \lambda/d$ with d the subaperture size. The bench must reproduce the correct ratio between the two sizes of the most elongated spot i.e.

$$E = \frac{\theta_{Na}}{\theta_{LGS}} = 10.72.$$

Moreover the elongated spot must be sampled with 14×14 pixels with a pixel scale given by $0.7\lambda/d$.

The elongated spot can be decomposed as the sum of independent non–elongated spot each with a different focus aberration.A focus optical aberration is given by

$$\varphi(r) = a_4 \left(\frac{r}{R_4}\right)^2, \tag{1}$$

with a_4 the focus amplitude in nm and R_4 the radius of the pupil on which the aberration is defined. The corresponding wavefront slopes is

$$\frac{\partial\varphi(r)}{\partial r} = 2a_4\frac{r}{R_4^2}, \tag{2}$$

The wavefront slopes corresponding to the most elongated spot on the bench is

$$\beta = \frac{E}{2}\frac{\lambda}{d} = 2a_4\frac{L}{R_4^2} \tag{3}$$

leading to

$$a_4 = \frac{E}{4}\frac{\lambda}{d}\frac{R_4^2}{L} \tag{4}$$

noting that $R_4 = L$ and $L = N_L d$, one finally obtains

$$a_4 = E\frac{\lambda}{4}N_L. \tag{5}$$

With $\lambda = 635\text{nm}$ and $N_L = 16$, the focus amplitude is $a_4 = 33\mu\text{m}$.

The principle of the elongation making on the bench is then to create an off–axis focus on the lenslet array of the WFS with an amplitude from -33μm to +33μm. The focus step has to be chosen such as the WFS spot moves of half a pixel or less per step. The brightness of the source must also be controlled synchronously with the focus sweep in order to write into the elongated spot the desired Na profile. The phase screens must be steady during the focus sweep. It is important to note that each LGS goes through a different portion of the phase screens depending on the desired LGS angular separation. This means that for each LGS the beam location on the phase screen has to be adjusted.

There are several methods to produce an off–axis focus on the sensor

1. a deformable mirror can be controlled to create an off–axis focus,[6]
2. a lens on a z–translation stage with its optical axis aligned with the launch telescope location,
3. an x,y and z moving source,
4. a lens on a z, θ_x, θ_y stage,
5. some combination of lens and source motions.

3.2.1 The LGS wavefront sensor

The sampling of the lenslet images on the detector must resemble as close as possible to the sampling on the LTAO WFS of the GMT, meaning that the ratio of the pixel scale to the spot FWHM must be close to 0.7, i.e.

$$0.7 = \frac{p}{\xi} = \frac{pd}{\lambda f} = \frac{p}{\lambda f_{\#}}. \tag{6}$$

From the former equation is derived the lenslet f–number

$$f_{\#} = \frac{10p}{7\lambda}. \tag{7}$$

Each lenslet image must be sampled with 14×14pixels.

3.3 Natural Guide Stars

Two natural guide stars should be added to the AO bench. One is on–axis and is used to assess the image quality by making an image after the segmented pupil. The second NGS is off-axis and it is used to estimate the tip and tilt components of the atmosphere as the tip–tilt measured by the LGS WFS will be discarded like on the on–sky LTAO system. As for the GMT LTAO system, the off–axis NGS should be AO corrected with a DM on its path after the segmented pupil. The correction order should be less that the correction order of the on–axis DM. The same off-axis NGS should be used to test the Na mean altitude tracking loop and truth sensor loop. The effect of pupil rotation on the truth sensor should also be investigated with the off–axis NGS.

4. THE DESIGN

The schematic of the conceptual design is given in Fig. 2. The bench uses only one source to create the 3 LGSs in series. A dedicated scheduler will have to be written to ensure that the relative time constants on the bench match the same relative time constant of the GMT LTAO system. The main subsystems are detailed in the following sections.

4.1 The sources

There are 3 sources on the bench, 1 for the LGS and 2 for the on–axis and off–axis NGS. Each source must be of a different wavelength as dichroics are used to merge and separate the light beams from the different sources. The LGS wavelength has been chosen to be 635nm, the wavelength of the two other source must be chosen based on the spectral sensitivity of their respective detectors. Most of visible detector have a sensitivity typically better than 50% in the range [400–700]nm. The sources are temperature stabilized and the intensity is adjustable using an external signal.

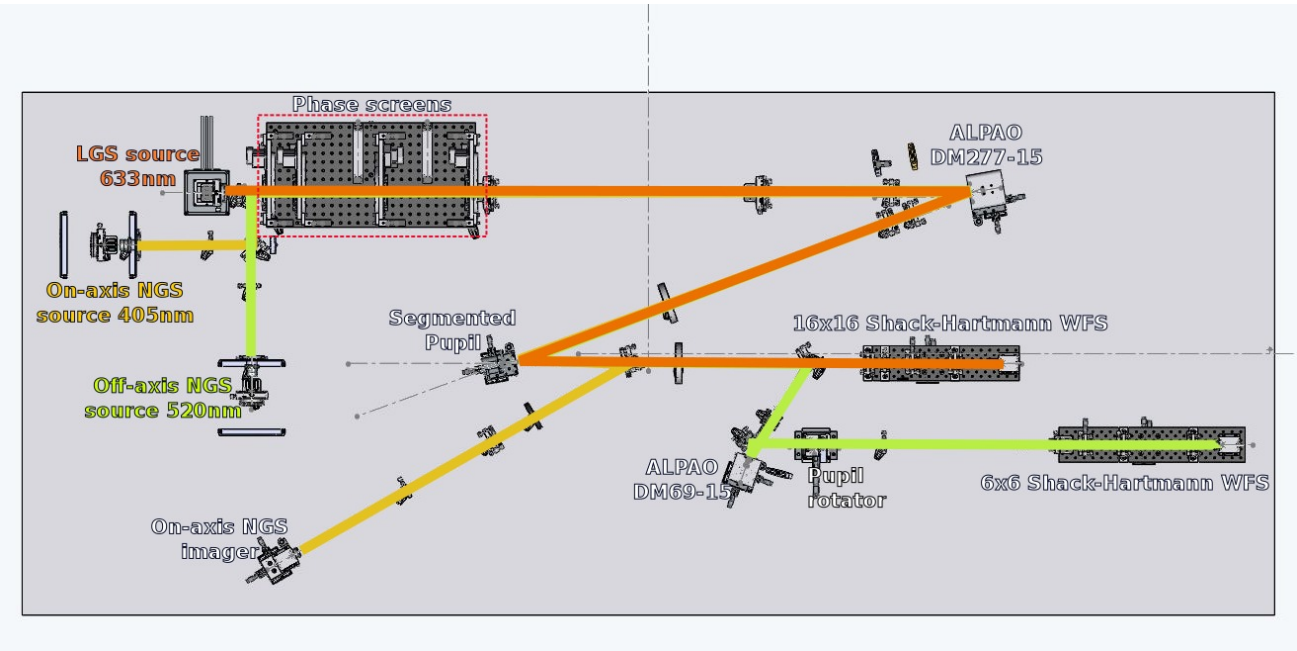

Figure 2. The opto–mechanical design of the LTAO bench

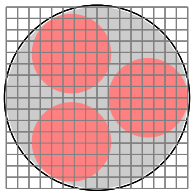

Figure 3. The 24mm diameter bench pupil (gray area) inside the DM clear aperture drawn at a 1:1 scale, with on top the segmented pupil and the 16×16 lenslet array.

4.2 Segmented deformable pupil

Trying to emulate the GMT ASM with individual DM is a costly solution. Instead we propose to use a single DM with a segmented pupil. A simple segmented mask will not allow testing the phasing techniques. So it is replaced by individual mirrors, each with its own tip–tilt and (x,y,z)–translation stage. This means that on the bench, the pupil needs to be relayed at least at two locations, one to host the continuous DM and the other to host the segmented mirror.

The DM is the Hi–Speed DM277-15 from ALPAO with 19 actuators across the diameter with a pitch of 1.5mm. The DM clear aperture is 24.5mm meaning that a 24mm pupil will fit into the DM aperture with exactly 17 actuators across the diameter. A 16×16 lenslet array is optically conjugated to the pupil and registered to the DM actuators according to the Fried geometry.

If we were matching the 7 segments of the GMT pupil onto the pupil of the bench, this will lead to 5 actuators per segment. This is a bit short with regards to the fitting error so we are opting for a 3 segment solutions (Fig. 3), each with $\simeq 8$ lenslets across. The schematic of the segmented mirror is given in Fig. 4 where 3 25mm diameter mirrors are evenly positioned on a 32mm diameter circle. The location of the launch telescope is also shown on the same diagram, there are located on a 42mm diameter circle similarly to the GMT. The point–spread function corresponding to the pupil of Fig. 4 is shown in Fig. 5.

4.3 The atmosphere model

To test both the performance of tomography algorithms and accuracy of C_n^2 profiling methods, we propose to use a 3 layer profile which parameters are given in Table 1. The anisoplanatic angle and decorrelation time for this profile are $\theta_0 = 5.8$" and $\tau_0 = 8.60$ms compared to $\theta_0 = 5.7$" and $\tau_0 = 8.15$ms for the GMT model.

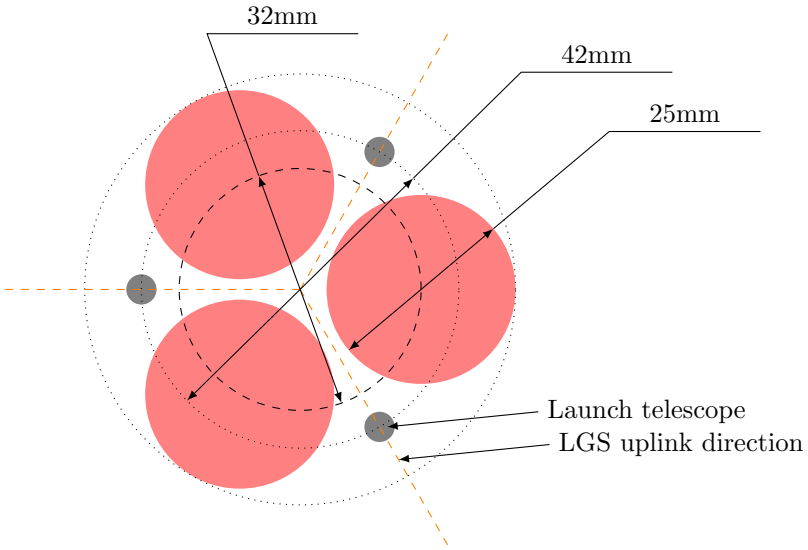

Figure 4. Pupil definition

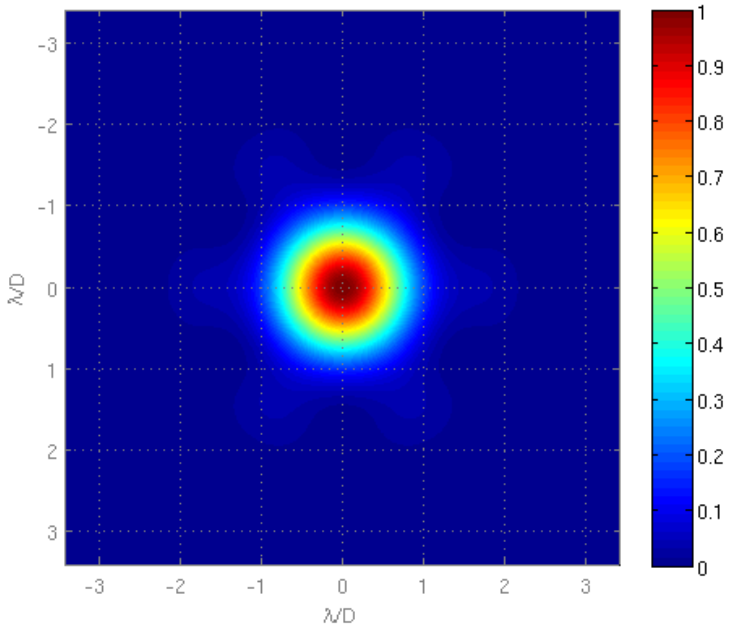

Figure 5. Diffraction limited image.

Layer	Altitude[m]	Weight	Wind speed [m/s]
1	1000	0.3	6
2	2500	0.5	12
3	10000	0.2	25

Table 1. Atmosphere profile.

Layer	Distance to pupil[cm]	r_0[mm]	Angular speed[arcmin/step]
1	20	1.19	1
2	50	0.88	2
3	200	1.52	5

Table 2. Phase plate parameters.

To reproduce the atmosphere profile given in Table 1, 3 rotating phase plates from Lexitek are used. The pupil diameter on the phase plate is $D_{atm} = 20$mm. The DM pitch on the phase plate is $d_{lab} = D_{atm}/16 = 1.25$mm leading to $r_{0,lab} = 0.58$mm in order to match $d/r_0(\lambda_{lab}) = 2.15$ (Sec. 3.1). The bench is emulating a 25.785m diameter telescope with a 1.6m DM pitch. On the bench $\mathcal{L}_{0,lab} = 46.5$mm in order to match the $D/\mathcal{L}_0$ of the GMT. The parameters of the phase plate are given in Table 2. The wind speed has been converted in rotation angle per step. Each step corresponding to a 2ms time lag. The conversion from wind speed to angular speed is given by

$$v_\theta = \frac{v}{d_{PL}} \frac{D_{atm}}{D} \frac{1}{500} \tag{8}$$

with $d_{PL} = 29.2$mm the distance from the rotation axis of the phase plate to center of the etched area, $D = 25.785$m the diameter of the equivalent telescope. The layout of the 3 phase plates is given in Fig. 6. It assumes a 20mm diameter pupil at the ground level and that the 10km phase plate is 20cm away from the pupil.

4.4 Laser Guide Stars

Fig. 8 plots the tomographic wavefront error as a function of the LGS constellation radius for 3 and 4 LGS evenly located on a ring. The tomographic error has been computed for a 25.785m diameter telescope, a 17×17 DM and the atmosphere profile of Table 1. 3 LGSs on 32" diameter circle have been selected. On the bench, the non elongated spot size is given by the lenslet diffraction limit, i.e. $\theta_{LGS} = \lambda/d$ with d the subaperture size and like on the detector of the LTAO WFS of the GMT, each imagelets is sampled with 14×14pixels. For a 25.785m diameter telescope with the launch telescope located as draw in Fig. 4, the longest distance from the pupil edge to the launch telescope is $L = 22.721$m. To produce a 10.72" LGS elongation, the thickness and distance to the Na layer needs to adjusted to $\delta_{Na} = 17.5$km and $h_{Na} = 87.5$km.

Creating several LGS–like sources simultaneously is certainly feasible but will involve a complex optical layout. Instead the elongation pattern corresponding to the 3 LGSs is made in series on a single WFS, the software is in charge to restore the correct time line for the tomography computation. A single source with fine control on its x, y and z displacement is chosen as the mean to produce the elongation on the sensor. The source also have to be moved to 3 different nominal position equivalent to a 16" arcsec angular displacement in the sky.

4.4.1 The LGS asterism

The LGS asterism is made by moving the LGS source off–axis of the distance $\delta_s = f\theta_s$, with f the focal length of the collimation lens. The bench must reproduce the beam footprint of a $\theta_{LGS} = 16$" off–axis LGS on an atmosphere layer at $h = 10$km. For a phase plate $z = 20$cm away from the pupil, the corresponding angular deviation of the beam is

$$\theta_s = \theta_{LGS} \frac{h}{z} \frac{D_{atm}}{D} = 0.17\text{deg}, \tag{9}$$

with $D = 25.785$m and $D_{atm} = 20$mm is the pupil diameter on the bench, leading to

$$\delta_s = \theta_{LGS} f_\# D_{atm} \frac{h}{z} \frac{D_{atm}}{D}. \tag{10}$$

For $f_\# = 2$, one finds $\delta_s = 120\mu$m.

The beam lateral displacement δ_{beam} on a phase plate at a distance z from the pupil is given by

$$\delta_{beam} = \theta_s z = \theta_{LGS} h \frac{D_{atm}}{D}. \tag{11}$$

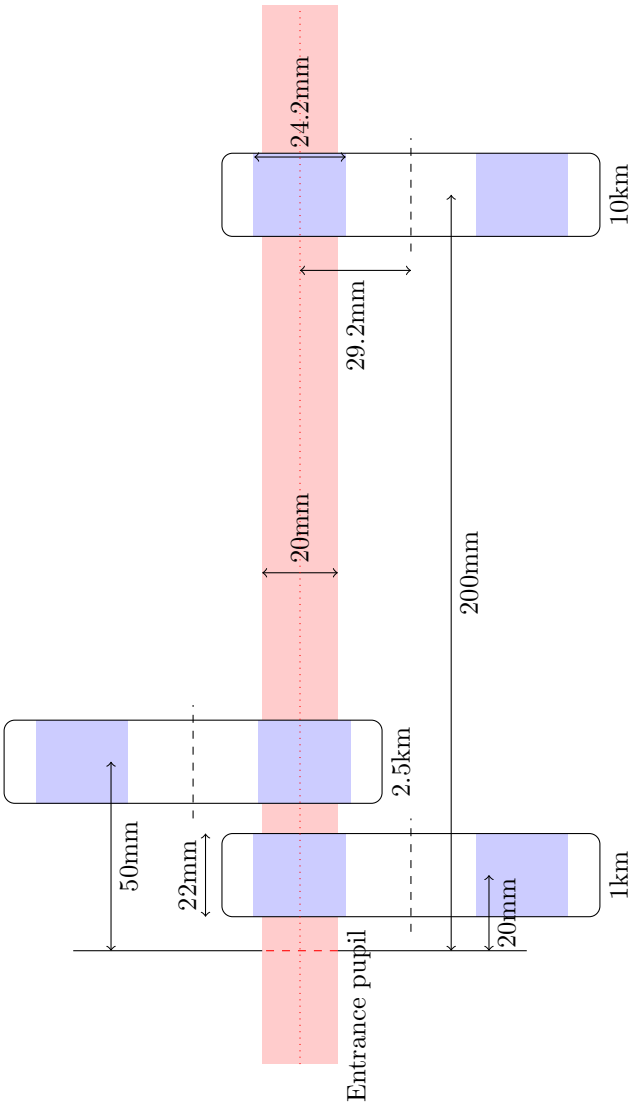

Figure 6. Phase plates layout.

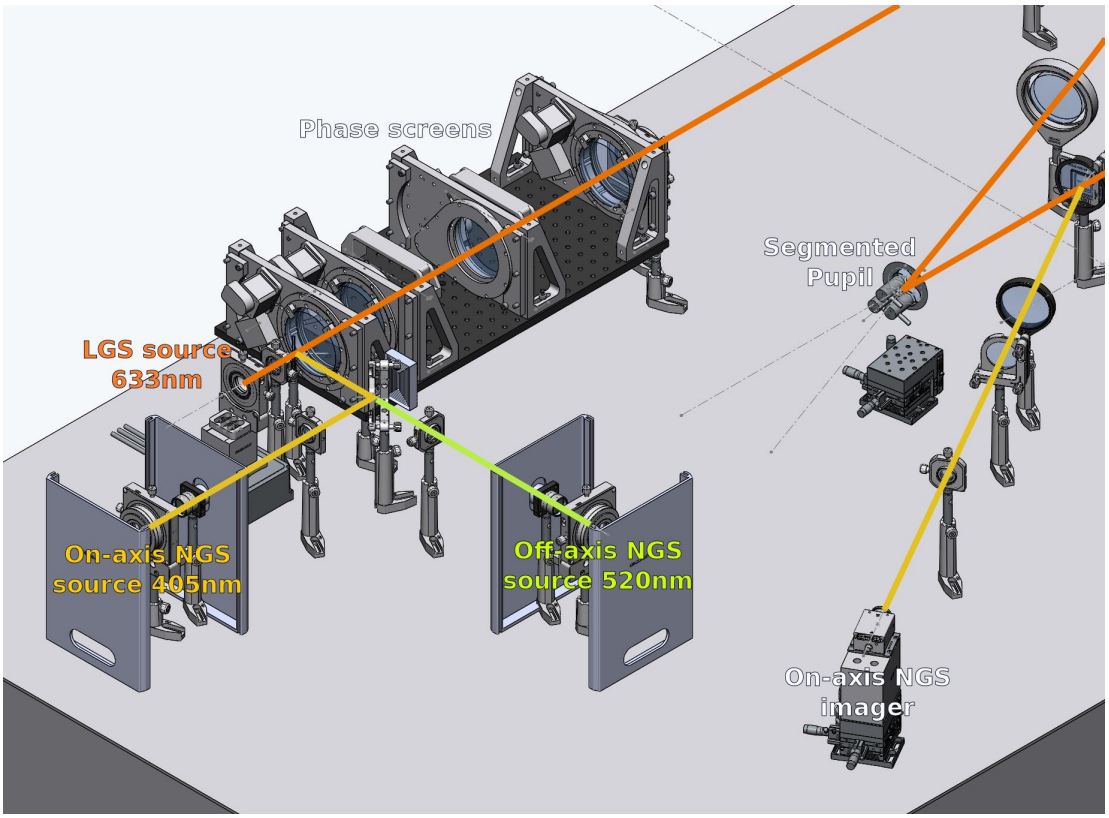

Figure 7. The front of the opto–mechanical design of the LTAO bench with the 3 sources, the phase screens, the segmented pupil and the on–axis source camera.

The largest beam displacement achievable on the bench is $\max(\delta_{beam}) = 2.1$mm according to Fig. 6. This set the field of view to

$$\theta_{fov} = 2\frac{\max(\delta_{beam})D}{hD_{atm}} = 111\text{arcsec.} \tag{12}$$

4.4.2 The cone effect

For the GMT, the optical rays from the LGS to the telescope pupil are slanted with an angle given by

$$\xi = D/2h_* \tag{13}$$

with $D = 25.785$m and $h_* = 90$km. The diameter of the telescope projected at altitude h is:

$$D_h = D\frac{h_* - h}{h_*} \tag{14}$$

The same relation must also hold for the LTAO bench.

On the bench, we are free to choose ξ^{bench} such as the experiment dimensions fit on the optical table. This sets the LGS altitude for the bench at:

$$h_*^{bench} = D_{atm}/2\xi^{bench} \tag{15}$$

with $D_{atm} = 20$mm. The altitude of the atmospheric layer must be adjusted accordingly:

$$D_h = D\frac{h_* - h}{h_*} = D\frac{h_*^{bench} - h^{bench}}{h_*^{bench}} \tag{16}$$

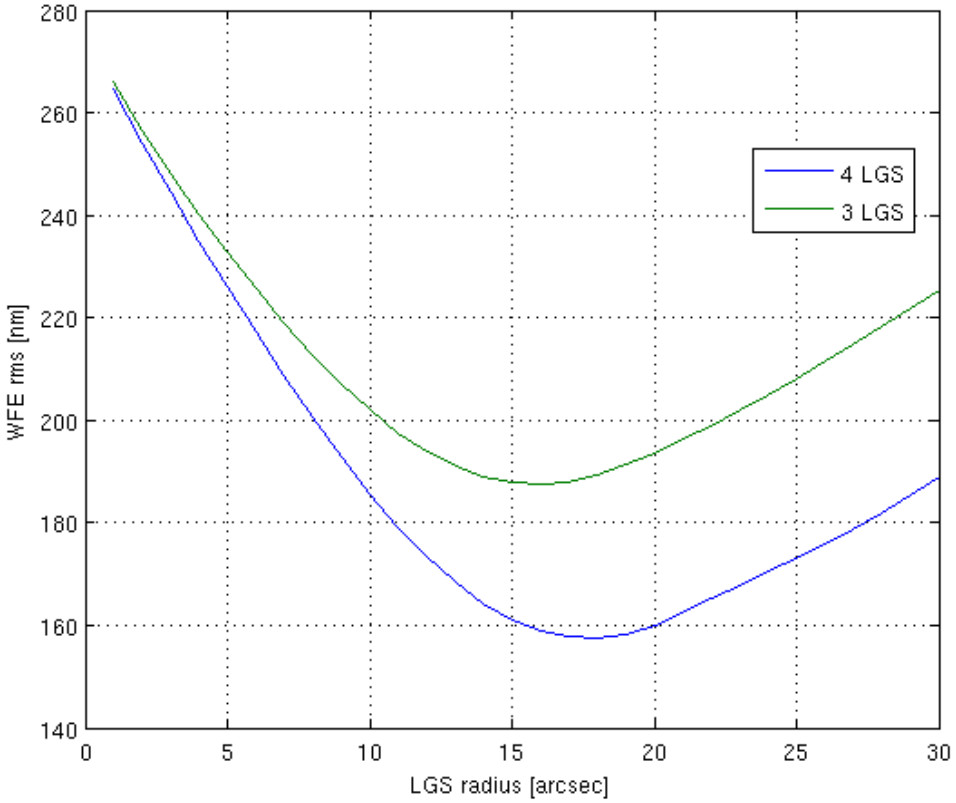

Figure 8. Tomographic wavefront error as a function of the LGS constellation radius for 3 and 4 LGS evenly located on a ring.

leading to

$$h^{bench} = h_*^{bench} - \frac{h_*^{bench}}{h_*}(h_* - h). \tag{17}$$

Setting $\xi^{bench} = \beta\xi$ with $\beta \geq 1$ and inserting Eq. (15) into Eq. (17) gives

$$h^{bench} = \frac{D_{atm}}{\beta D}h. \tag{18}$$

For $\beta = 1$ and $h = 10$km, we find $h^{bench} = 7.8$m.

4.4.3 Off-axis focus projection

The elongated spots are generated from a series of off–axis focus. This off–axis focus can be decomposed into an on–axis focus and a tip–tilt induced by moving the single LGS source along its x, y and z axis. The amplitude of the on–axis focus and tip–tilt are derived below. The wavefront on the WFS is given by

$$\varphi(\vec{r}) = a_4 \left| \frac{\vec{r} - \vec{r}_L}{R_4} \right|^2 = a_4\gamma_4 \left| \vec{\rho} - \vec{\rho}_L \right|^2 \tag{19}$$

with $\vec{r}_L$ the location of the launch telescope, R_4 the focus radius and $\gamma_4 = (R/R_4)^2$, R is the pupil radius. The coefficients b_i of the projection of the wavefront onto the Zernike polynomials are written

$$b_i = \frac{1}{\pi}\int_0^{2\pi} \mathrm{d}\theta \int_0^1 \mathrm{d}\rho\rho\varphi(\vec{\rho}R)Z_i(\vec{\rho}), \tag{20}$$

with $Z_i(\vec{\rho})$ the Zernike polynomials given by

$$Z_i(\vec{\rho}) = \alpha_{nm} R_n^m(\rho)\cos(m\theta_\rho + \beta_{im}) \tag{21}$$

with

$$\alpha_{nm} = \sqrt{n+1}2^{-\frac{1}{2}(\delta_{m0}-1)},$$
$$\beta_{jm} = \frac{\pi}{4}(1-\delta_{m0})\left[(-1)^j - 1\right]$$

and

$$R_n^m(\rho) = \sum_{s=0}^{(n-m)/2} g(s,n,m)\rho^{n-2s}, \quad g(s,n,m) = \frac{(-1)^s(n-s)!}{s!\left[(n+m)/2-s\right]!\left[(n-m)/2-s\right]!}$$

Inserting Eq. (19) and Eq. (21) into Eq. (20) leads to

$$b_i = 2a_4\gamma_4\alpha_{nm}\sum_{s=0}^{(n-m)/2} g(s,n,m)\begin{cases} \frac{1}{n-2s+4} + \frac{\rho_L^2}{n-2s+2}, m=0 \\ \frac{\rho_L}{n-2s+3}\cos\left(\beta_{jm}+\theta_L\right), m=1 \\ 0, \forall m > 1 \end{cases} \tag{22}$$

From the Eq. (22), the tip, tilt and focus coefficients are derived

$$b_2 = a_4\gamma_4\rho_l\cos(\theta_L) \tag{23}$$
$$b_3 = a_4\gamma_4\rho_l\sin(\theta_L) \tag{24}$$
$$b_4 = a_4\gamma_4\frac{\sqrt{3}}{6}. \tag{25}$$

Assuming a pupil diameter D_{WFS} on the SH–WFS lenslet array, the launch telescope are located on a circle of diameter

$$r_L = (16/57)(11.5/8.71)D_{WFS}$$

and

$$R_4 = r_L + D_{WFS}/2,$$

leading to

$$\rho_l = 2r_L/D_{WFS} == 2(16/57)(11.5/8.71) = 0.74$$

and

$$\gamma_4 = \left(\frac{D_{WFS}}{2R_4}\right)^2 = \left(\frac{1}{\rho_L+1}\right)^2 = 0.33.$$

A tip and a tilt in the pupil corresponds to an x and y motion in the image plane with an amplitude of

$$\delta_{x,y} = \frac{2b_{2,3}f}{R_{WFS}} = 4b_{2,3}f_\# = 4a_4\left(\frac{1}{\rho_L+1}\right)^2\rho_l f_\#\begin{cases}\cos(\theta_L)\\ \sin(\theta_L)\end{cases} \tag{26}$$

and a focus correspond to a z displacement of amplitude

$$\delta_z = \frac{16\sqrt{3}b_4 f_\#^2}{1-16\sqrt{3}b_4 f_\#/D_{WFS}} = \frac{8\gamma_4 a_4 f_\#^2}{1-8\gamma_4 a_4 f_\#/D_{WFS}}.$$

With $f_\# = 2$ corresponding to a numerical aperture of approximately 0.25 and $D_{WFS} = 24$mm, the amplitude of the source motion is

$$\delta_{x,y} = \pm 65\mu\text{m}$$

and

$$\delta_z = \pm 351\mu\text{m}.$$

The range of motion in X, Y and Z directions should be swept in 40 steps. The LGS source motion in the x–y and x–y–z planes are shown in Fig. 9 and Fig. 10, respectively.

A suitable stage is the Nano–3D500 from Mad City Labs. The stage has a range of motion of 500μm in the 3 directions, a resolution of 1nm and a resonant frequency of 150Hz. Moreover it uses a closed–loop controller for absolute positioning. At a top speed of 15mm/sec, with this stage, 1 LGS can be generated in 25ms.

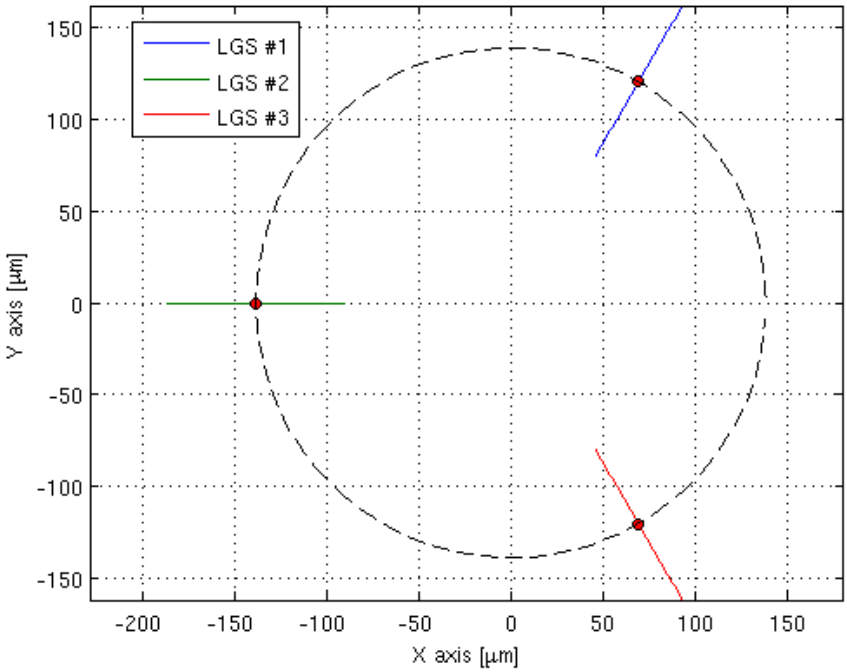

Figure 9. LGS source motion in the X–Y plane.

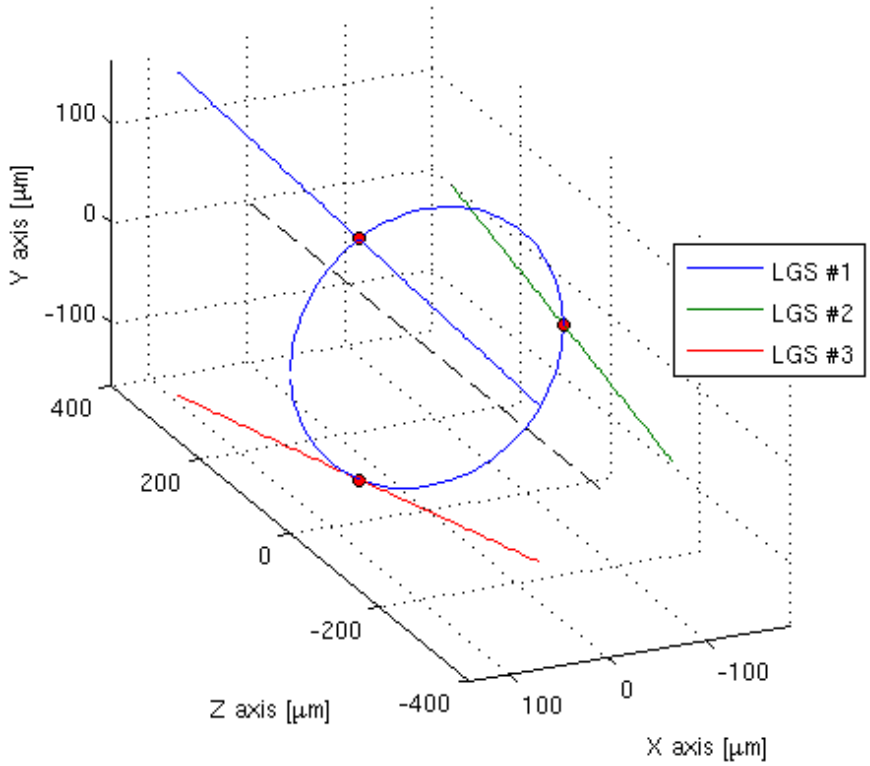

Figure 10. LGS source motion in the X–Y–Z plane.

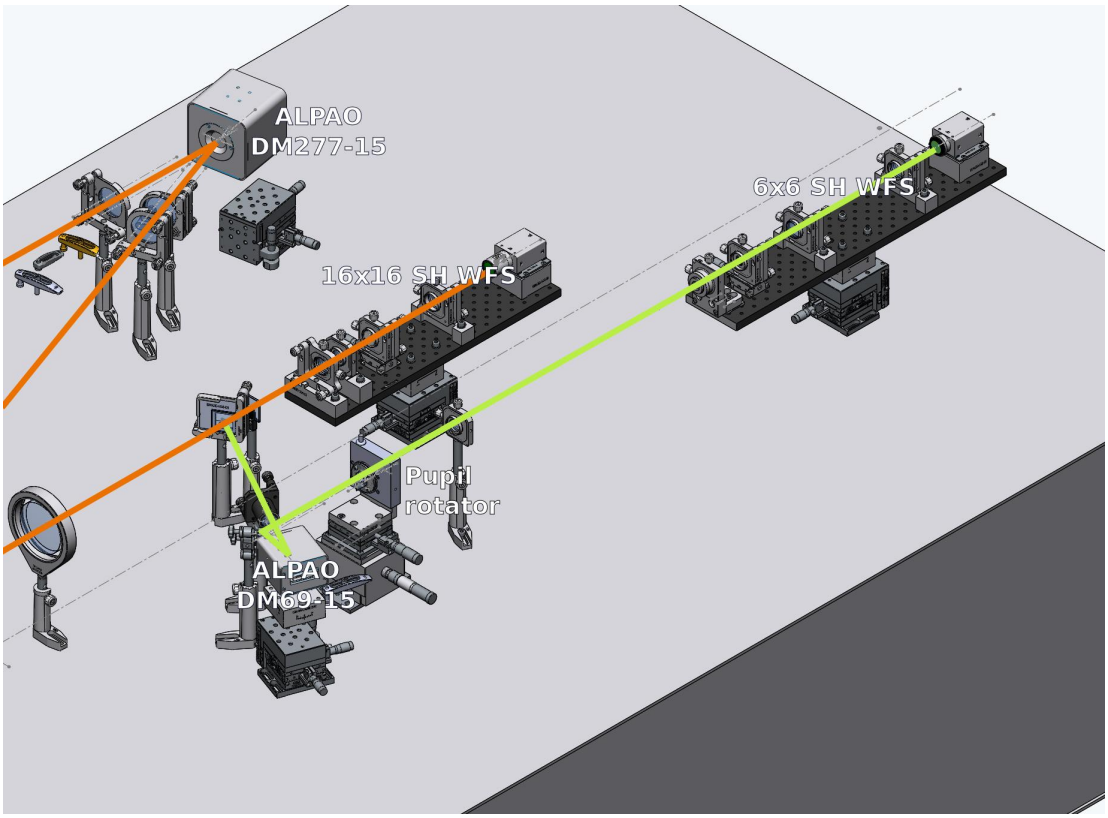

Figure 11. The back of the opto–mechanical design of the LTAO bench with the 2 DMS and the 2 WFSs.

4.4.4 The LGS wavefront sensor

The LGS WFS is a Shack–Hartmann sensor with a 16×16 lenslet array. The detector is the Grasshopper camera from Point Grey Research with a Sony KAI0340 CCD. The detector has a resolution of 640×480 pixels at 200 frames per second pixels with square pixel of size 7.4μm. From Eq. (7) with $p = 4.4\mu$m and $\lambda = 635$nm, the required lenslet f–number is $f_{\#} = 9.93$. The size of the LGS source, once imaged on the LGS WFS detector, must be smaller than the diffraction limit. i.e. $< \lambda f_{\#} = 6.61\mu$m. The centroiding window is 14×14 pixels per subaperture. A minimum of 2 guard pixels between adjacent subaperture is required. Simulated frames of the detector for the 3 LGSs are given in Fig. 12.

4.5 The Natural Guide Stars

Both NGS sources have a different wavelength which cannot be the same than the wavelength of the LGS source.

4.5.1 On–axis NGS

The on–axis NGS is injected just before the atmosphere subsystem and extracted after the segmented pupil to be focused on a camera to form an on–axis image to assess the performance of the LTAO system. The sampling of the image on the camera is such as there are at least 2 pixels across the FWHM of the diffraction limited image.

4.5.2 Off–axis NGS

The off–axis NGS is injected just before the atmosphere subsystem and extracted after the segmented pupil, then a pupil is form first on a second DM and finally on the lenslet array of the off-axis SH–WFS. The off–axis DM is an ALPAO Hi-Speed DM69–15. A 6×6 lenslet array is optically conjugated to the DM. The sampling of the image at the focal plane of the lenslet respect the Nyquist criteria i.e. 2 pixels across the FWHM. A dove prism is inserted prior to the lenslet array to induce rotation of the pupil. The detector is the same as the detector for the LGS WFS i.e. the Grasshopper camera from Point Grey Research.

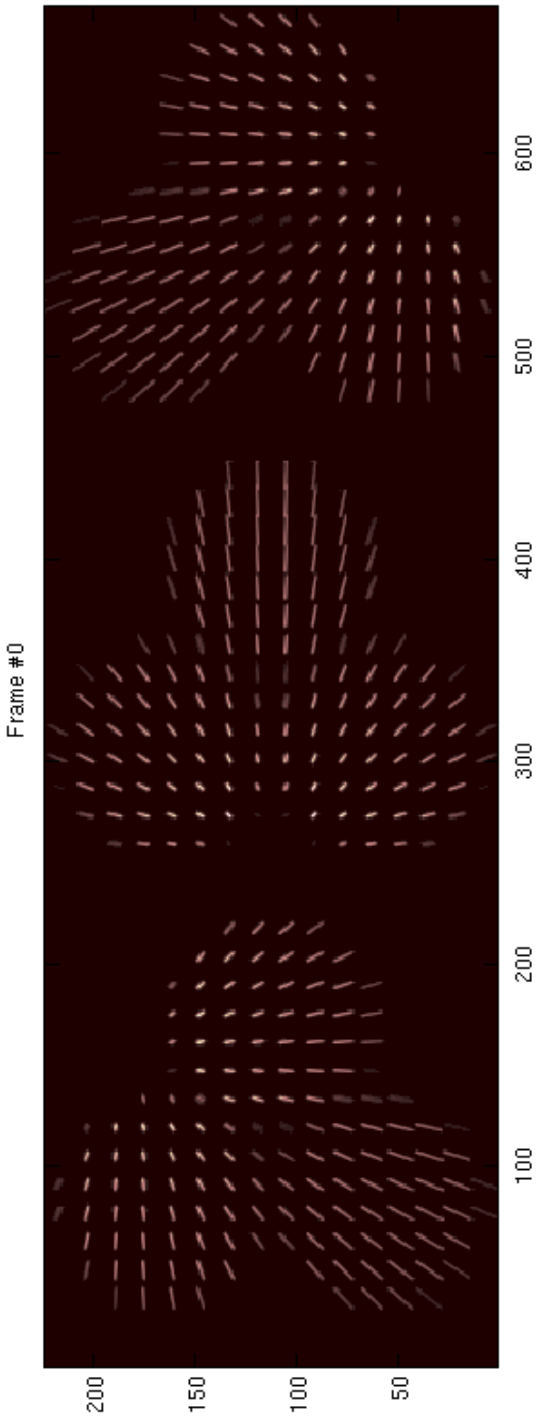

Figure 12. LGS WFS detector frames.

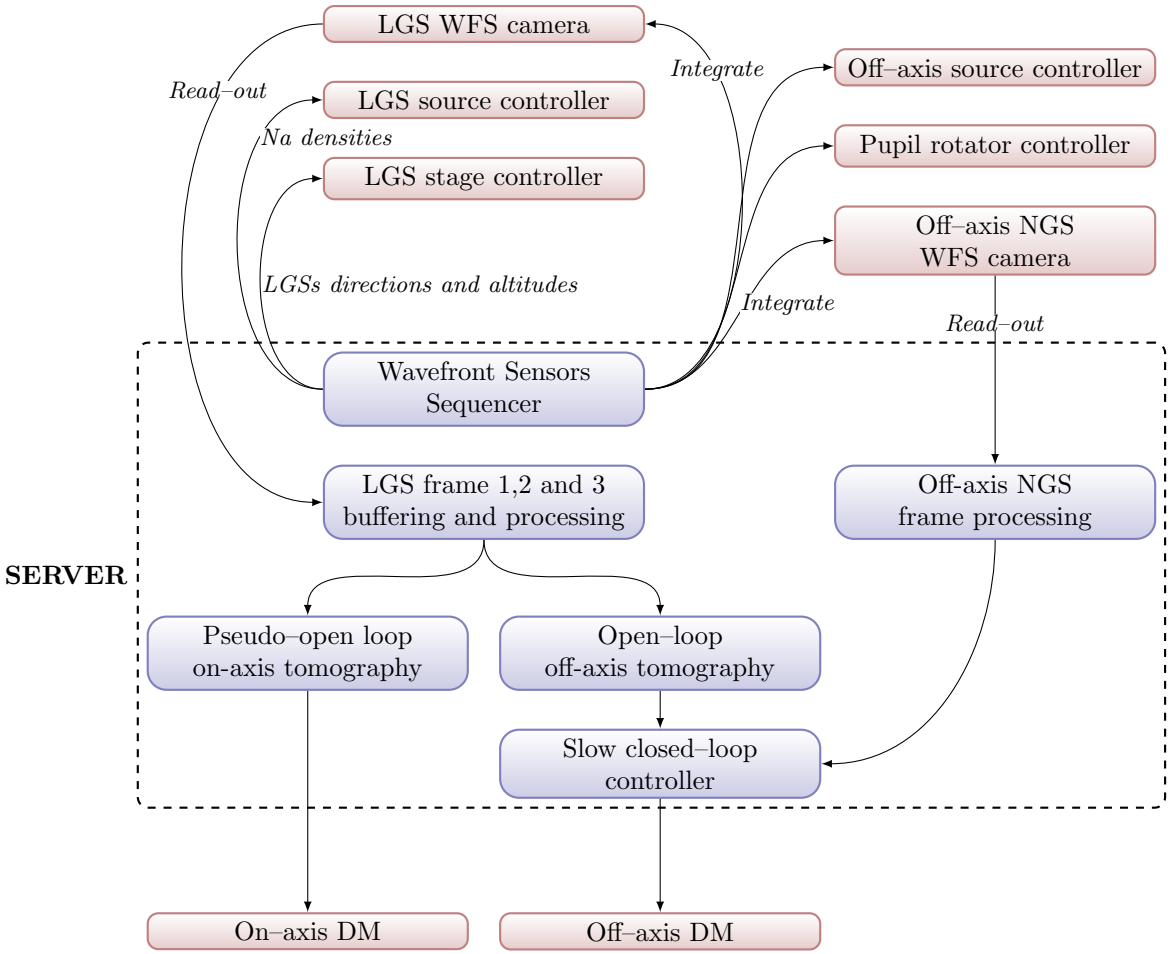

Figure 13. LTAO Test Bed block diagram

5. THE CONTROL

Fig. 13 shows the bench control diagram. The timing diagram is given in Fig. 14. The main sequence of events consists in generating 3 LGS frames corresponding to 3 LGS launch from 3 different locations at the pupil edge. This is done by simultaneously commanding the LGS stage based on the direction and altitude of the LGS and the LGS source intensity based on the Sodiun (Na) density profile. While the LGS stage and LGS source are updated, the LGS WFS camera is integrating hence recording the trace of the LGS source on the detector.

Once the 3 frames have been read–out from the LGS WFS camera, they are processed to extract the LGS WFS slopes that are used by both the on–axis and off–axis tomographic reconstructor to estimate the wavefront in both directions. A pseudo–open–loop controller is used for the on–axis DM. For the off–axis DM, the actuator command is derived from the open–loop LGS off–axis tomography estimate and from the closed–loop NGS off–axis estimate.

The rotation of both the phase screens and the pupil rotator are synchronized with the read–out of the LGS WFS detector.

6. CONCLUSION

A LTAO test bed for Extremely Large Telescope is being built in the Adaptive Optics laboratory of the Australian National University. The main features of the bench are:

- 3 LGSs with intensity profile variation,

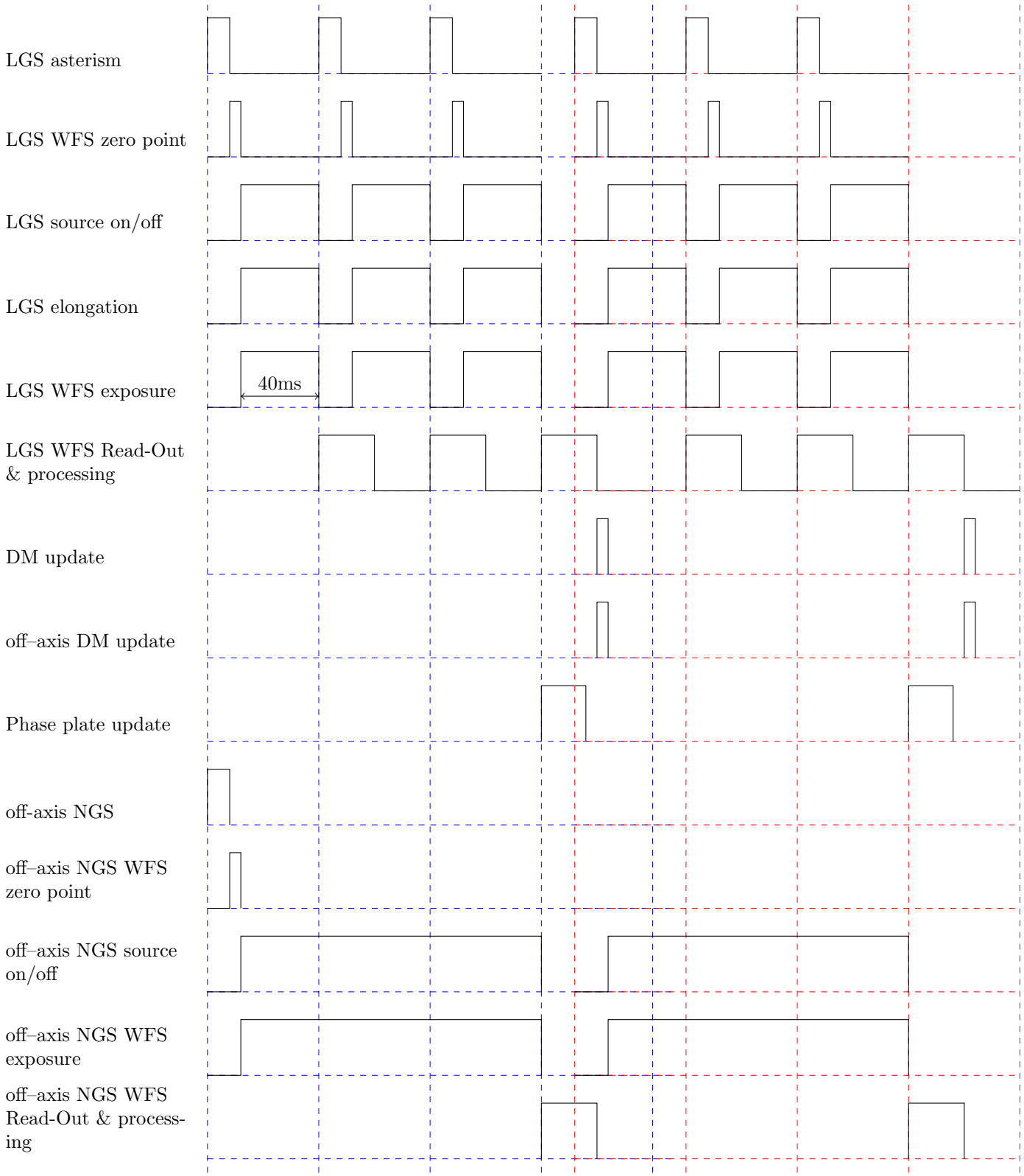

Figure 14. LTAO Test Bed timing diagram.

- 1 on–axis NGS,
- 1 off-axis NGS,
- 1 DM for on–axis correction,
- 1 DM for off–axis correction,
- atmosphere emulator with 3 layers,
- pupil rotation on off–axis optical arm.

The LTAO test bed went through a detailed design phase, the procurement of the required parts is well underway and the integration is starting.

REFERENCES

[1] A. Reeves, R. Myers, T. Morris, A. Basden, and N. Bharmal, "Real-Time Laser Guide Star Elongation and Uplink Turbulence in the Lab," in *Proceedings of the Third AO4ELT Conference*, S. Esposito and L. Fini, eds., Dec. 2013.

[2] S. M. Ammons, L. Johnson, R. Kupke, D. T. Gavel, and C. E. Max, "Laboratory demonstrations of LTAO on 30-m telescopes at visible wavelengths: Including multiple natural guide stars," in *Second International Conference on Adaptive Optics for Extremely Large Telescopes. Online at ¡A href="http://ao4elt2.lesia.obspm.fr"¿http://ao4elt2.lesia.obspm.fr¡/A¿, id.P12*, p. 12P, September 2011.

[3] O. Lardiere, R. Conan, C. Bradley, K. Jackson, and G. Herriot, "A laser guide star wavefront sensor bench demonstrator for TMT," *Opt. Express* **16**(8), pp. 5527–5543, 2008.

[4] R. Conan, , B. Espeland, S. Parcell, M. V. Dam, A. Bouchez, and P. Piatrou, "Laser Tomography Adaptive Optics for the Giant Magellan Telescope," in *Adaptive Optics for Extremely Large Telescopes III*, May 2013.

[5] F. Bennet, K. Uhlendorf, R. Gardhouse, R. Conan, B. Espeland, and A. Bouchez, "Integrated Optic Segment Piston Sensor for the GMT," in *Adaptive Optics for Extremely Large Telescopes III*, May 2013.

[6] R.Conan, O. Lardiere, G. Herriot, C. Bradley, and K. Jackson, "The TMT/NFIRAOS LGS wavefront sensing demonstration bench," in *Adaptive Optics for Extremely Large Telescopes*, June 2009.